Taking a Sneak Peek at Nature's Chemistry Notes on Photosynthesis

David Emanuel Elcock (Jr.)
Chemical Science - *23 36 98 44*
Summer 1 | *09/06 - 05/09 2025*

Trinity College Dublin
Coláiste na Tríonóide, Baile Átha Cliath
The University of Dublin

1 Introduction

A living cell utilises the energy currency called Adenine Triphosphate (ATP) in exchange for essential services such as mobility, protein synthesis and replication. In plants and several other species, ATP is made through a process called *photosynthesis* (Fig. 1). A key structure identified to facilitate this process is photosystem II (PSII), a protein complex that acts as a light-activated switch starting the process. Synthetically the biochemistry of PSII is challenging to reproduce in a laboratory due to the stability and inertness of water (H_2O). The strength of the O−H bond requires a reactive species to form which in PSII is achieved using light whose energy is funnelled to reaction center called P680. By mimicking the chemistry of this pigment, water splitting could become solar powered and help provide a clean energy source. In this report a mimic of P680 is investigated for insight into the challenging chemistry of PSII. By comparing the optical and electrochemical spectra against a control mimic the effects of cations are compared to test for the role of peripheral charges in describing the chemistry of P680.

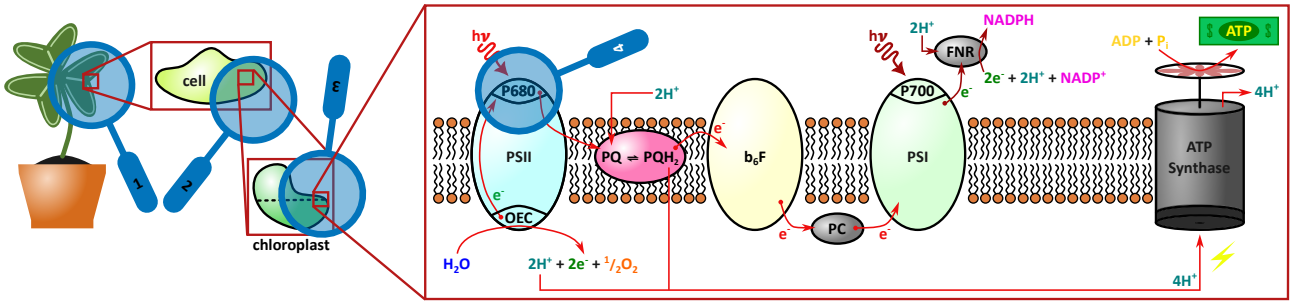

Figure 1: *Overview of Photosynthesis.*
Plants (1) consist of cells (2) containing organelles called chloroplasts (3). A series of protein complexes including photosystem II (PSII) generates the energy currency ATP, adenine triphosphate. Light around 680 nm oxidises (single electron loss) the P680 reaction center to $P680^{\cdot+}$ which oxidises the oxygen evolving complex (OEC) where for water splitting. The transferred electrons from water are ferried through plastoquinone (PQ), an intermediate complex (b_3F) and plastocyanin (PC) before reaching photosystem I (PSI). Here a second light excitation around 700 nm excites the electron to a higher energy state. A ferredoxin-$NADP^+$ reductase (FNR) enzyme uses the excited electron to drive the synthesis of an electron and proton shuttle molecule (NADPH) which is used in the Calvin cycle for sugar synthesis. The build-up of a proton gradient across the membrane by these processes is used to drive the conversion of adenin diphosphate (ADP) to adenin triphosphate by the ATP synthase protein complex.[1]

2 Theory

The biochemical synthesis of glucose (sugar) and oxygen (O_2) via *photosynthesis* is divided into two parts, a light-dependent breakdown of water and light-independent (dark) synthesis of sugars. Whilst the chemistry of the dark reaction is known, the light reaction remains elusive for several reasons. PSII is a large structure, is difficult to isolate or synthesise and exhibits different physical properties to its components: four chlorophyll-*a* (Fig. 2).

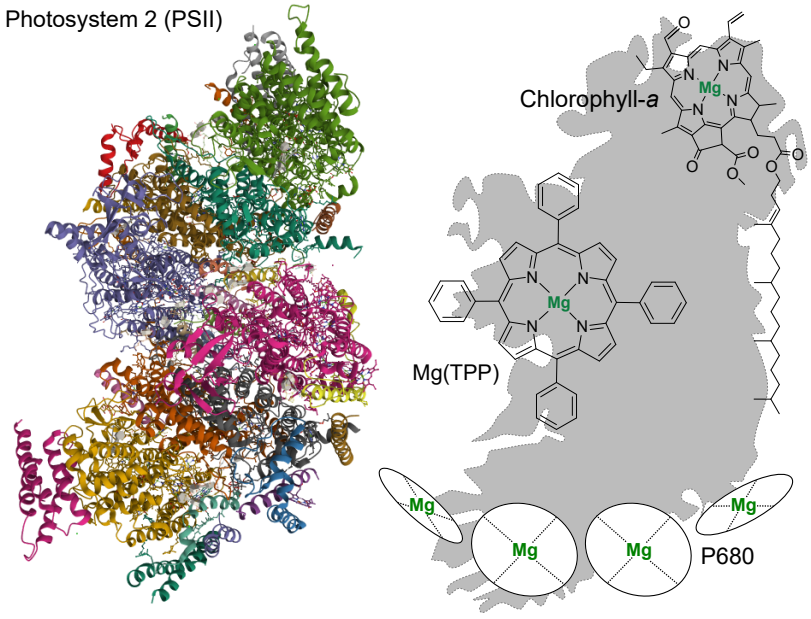

Figure 2: *Photosystem II Mimics.* Photosystem II with proteins labelled by colour.[2] The chlorophyll-*a* unit of the P680 reaction center is shown along with their arrangement. An examples of a mimic molecules (MgTPP) is shown.

The reactivity seen in PSII is made possible through the tuning of electron transfer properties (ET) of P680. In particular, the measure of ease at which electrons are transferred from/to a chemical species, the redox potential E^o differs between a single chlorophyll-*a* to chlorophyll-*a* in P680. Whilst the redox potential for a molecule is expected to be a constant, chlorophyll-*a* shifts from 0.8 V to 1.3 V. The leading hypothesis for this shift considers the effects of peripheral charges surrounding the P680.[3] A static electric field by ions from the protein backbone and the vicinity of adjacent chlorophyll-*a* molecules is suspected to induce beneficial energy level shifts by a quantum-mechanical phenomenon called the *Stark* effect. To verify this hypothesis a novel mimic was synthesised[a] to which metal cations can be bound - mimicking the peripheral charged environment P680 is exposed to (Fig. 3). This mimic builds on previous work by increasing proximity which is expected to increase the tuning of the ET properties.[4] By varying the metal cation used the effect of charge density magnitude (charge and radius) can be probed.

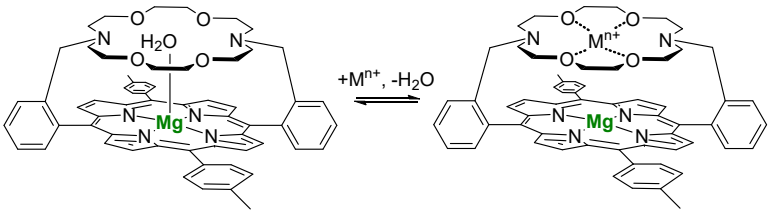

Figure 3: *Chlorophyll-a Mimic.* Chlorophyll mimic relevant to this study named *'MgCrown'*. This is synthesised by Oscar Reid Kelly.

2.1 Synthesis of Porphyrins

To investigate reaction centers, synthesis commences with the ligand, the organic molecule that surrounds a metal ion (Mg^{2+} for chlorophyll). A simple mimic ligand is tetraphenylporphyrin (H_2TPP). Due to its symmetry it can be synthesised by refluxing pyrrole (C_4H_5N) with benzaldehyde (C_7H_6O), a process that involves the continual heating of the volatile reaction mixture whilst cooling the vapour to prevent solvent loss. The reaction is sped up using propionic acid (CH_3CH_2COOH) and oxygen as catalysts (fig. 4). After a work-up, a series of purifying/isolating steps the ligand can be complexed with a metal via a metalation reaction.

$$4\,C_4H_5N_{(l)} + 4\,C_7H_6O_{(l)} \xrightarrow[3/2\ O_2]{CH_3CH_2COOH} H_2TPP_{(s)} + 7\,H_2O_{(l)} + \text{other polymers}_{(l)}$$

$$H_2TPP_{(sln)} + MgBr_2 \cdot OET_{2(sln)} \xrightarrow[NEt_3]{} MgTPP_{(s)} + 2\,HNEt_3{}^{+}Br^{-}_{(sln)} + OET_{2(sln)}$$

[a] Synthesis of the novel mimic was by Oscar Reid Kelly from the McDonald Group at Trinity College Dublin

The non-complexed ligand (H_2TPP free-base) is complexed with magnesium by forming a solution of H_2TPP and magnesium bromide etherate ($MgBr_2 \cdot OEt_2$) in dichloromethane (DCM) as solvent. The reaction is catalysed by triethylamine NEt_3 producing the MgTPP complex, the magnesium complexed P680 mimic. Since the reaction produces the acid HBr as a by-product, NEt_3 also prevents protonation of MgTPP into its free-base H_2TPP via acid-case neutralisation. Work-up isolates MgTPP from the side-products. Synthesis of the MgCrown (fig. 3) by Oscar Reid Kelly follows a similar approach with a more elaborate work-up.

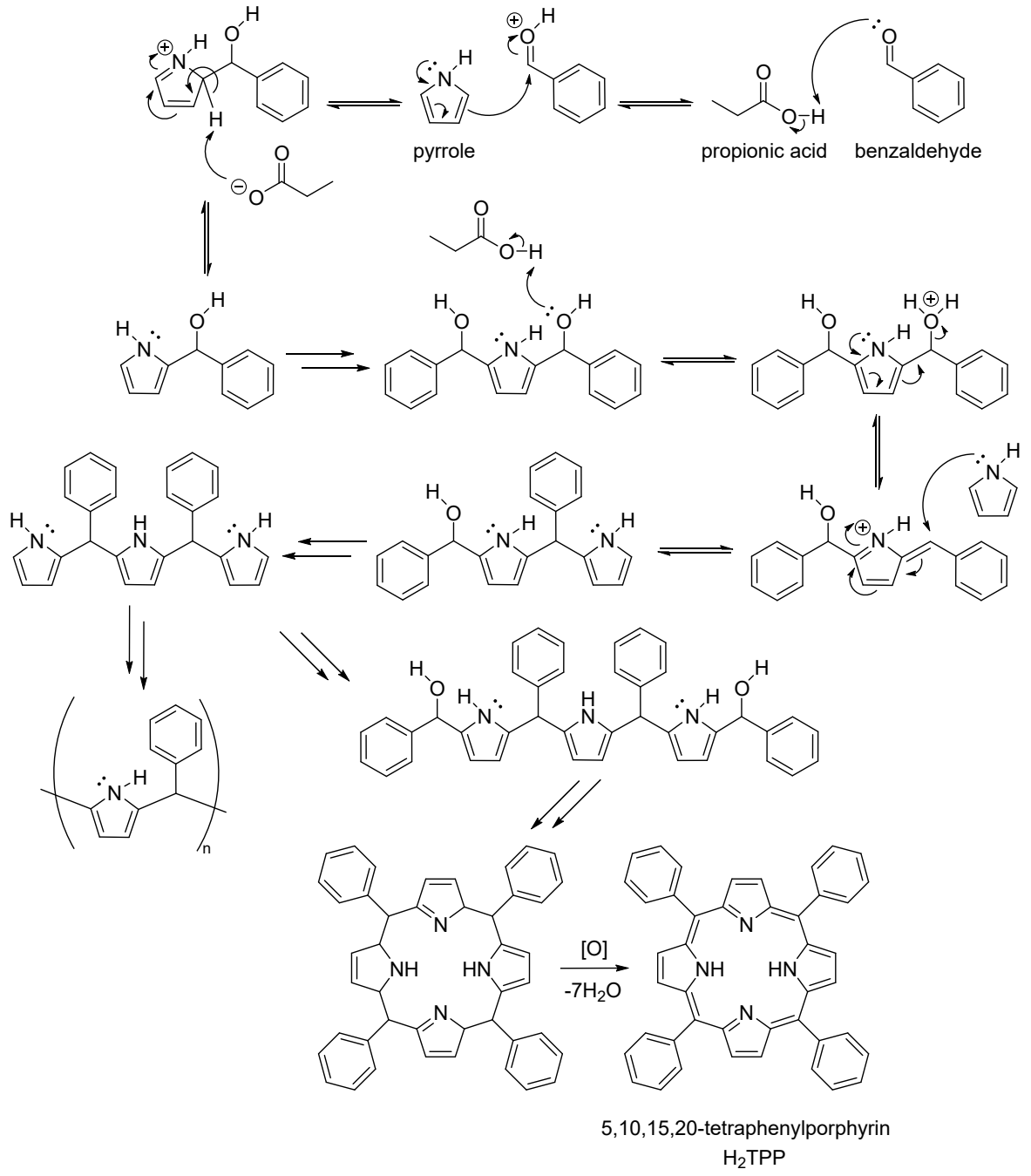

Figure 4: *Free-base Synthesis.*
Reaction mechanism for the synthesis of H_2TPP (Free-base). Proprionic acid catalyses the binding of benzaldehyde to pyrrole forming a polymer. A fraction of 4 nitrogen long monomers undergoes ring closure which upon oxidation forms the ligand H_2TPP. The net reaction is given by: $4\,C_4H_5N(l) + 4\,C_7H_6O(l) \xrightarrow[3/2\ O_2]{CH_3CH_2COOH} H_2TPP(s) + 7\,H_2O(l)$ + other polymers(l).

2.1.1 Tracking Reaction Progress

To ascertain the formation of a product, two techniques are used in this work: proton nuclear magnetic resonance (^{1}H NMR) and infra-red spectroscopy (IR). These techniques allow for identifying species in a sample and determine impurities.

^{1}H NMR probes proton environments in organic molecules placed in a strong magnetic field. Every proton environment - like an carboxylic acid, amine , etc. starts to behave as a magnet that either aligns with or against the external applied magnetic field. Due to quantum mechanical effects, different proton environment acquire different resonances which can be used to identify parts of a molecule. Tracking the formation of an organic product is made possible through identifying the proton environments present in the molecule (1D) and the relative relationship of these environments between the environments (2D). For simple porphyrin[b] ligands like chlorophyll the verification is possible using 1D ^{1}H NMR (Fig. 5).

Infra-red uses electromagnetic radiation in the infra-red part of the spectrum to excite vibrations in the molecule. Different bonds have different characteristic vibrations that can be influenced by the surroundings of the molecule. Intermolecular bonding can broaden a peak and different bond strengths will appear at different energies proportional to the wavenumber (Fig. 5).

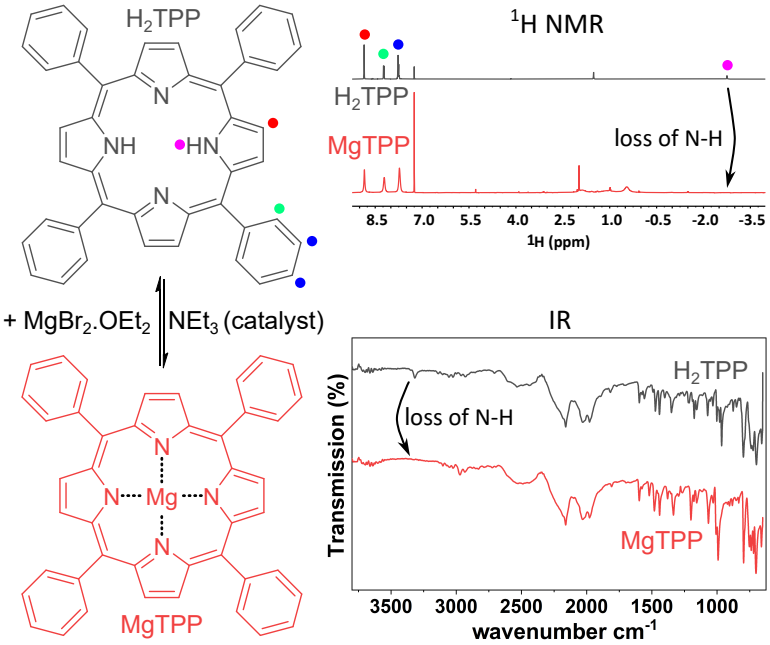

Figure 5: *Verify Metalation.* The metalation from H_2TPP to MgTPP can be checked for organic impurities with proton nuclear magnetic resonance (NMR) and infra-red (IR). The loss of the N-H proton environment removes the resonance from the ^{1}H NMR spectra with additional peaks identifiable as solvent, acetone, water and grease. The loss of the vibrational stretch of the N-H bond without the broadening of O-H bonds affirms metalation and shows the product is dry.

2.2 Analytical Techniques

To quantify the tuning of the ET properties both the redox potential and the optical transitions of the mimic complexes are investigated. Any changes to the redox potential can be measured using cyclical voltammetry (CV). This electrochemical technique applies a voltage to a solution containing redox-active chemical species and measures the electrical response (current) as a response to the applied voltage (Fig. 6). Optical transitions can be measured using ultraviolet-visible spectroscopy (UV-VIS). A light source with a tunable wavelength is made incident on a solution containing the species, exciting optical transitions (Fig. 7). Depending on how ET tuning by peripheral charges affects the electron energy-levels of the ground and excited states of the mimic both CV and UV-VIS provides a general overview of ET tuning (Fig. 8).

[b] Family of related species that includes chlorophyll and the mimics.

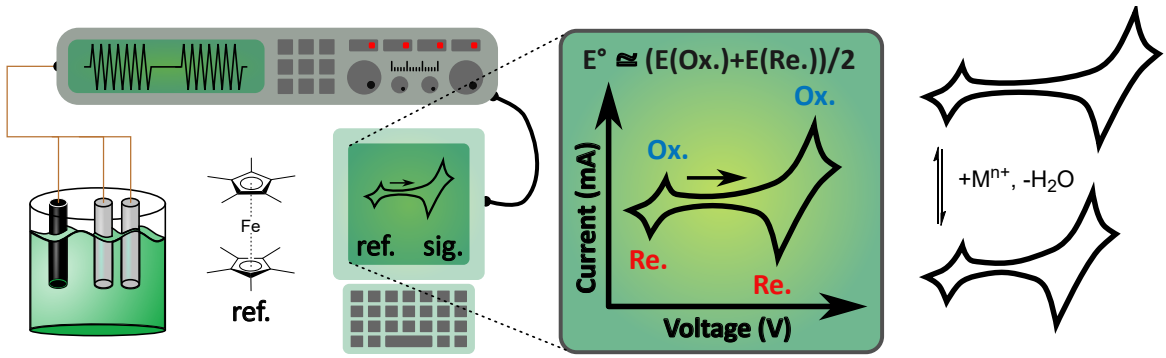

Figure 6: *CV Instrument.*
Cyclical Voltammetry (CV) makes use three electrodes: working, counter and reference. The working such as a glassy carbon electrode tracks the electrical flow of current due to the applied voltage on the system. The counter electrode closes the circuit whilst the reference defines the voltage to a common scale. Reference electrodes typically use cationic membranes which could affect the measurements hence a platinum wire is used (identical to the counter). Decamethylferrocene is thus used as an alternative reference (ref.) to reference the peak oxidation (ox.) and reduction (re.) peaks. For the signal (sig.) from the mimic the process of metal insertion could shift, indicating a shift in redox potential E°.

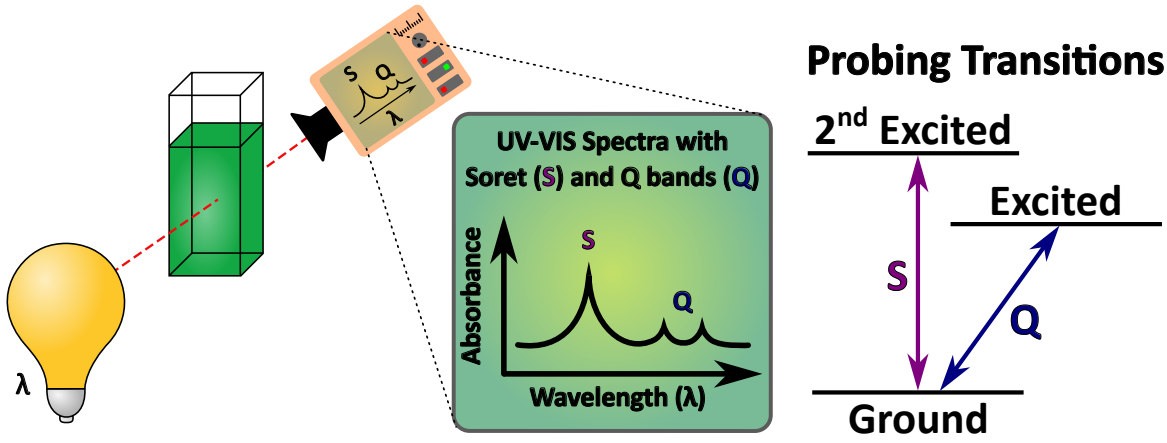

Figure 7: *UV-VIS Instrument.*
Ultraviolet-Visible Spectroscopy (UV-VIS) probes chemical species using light. For porphyrin ligands two types of bands appear, an intense soret singlet (S) and dimmer Q bands (Q). The bands differ in the excited state the electron is excited to with the Q bands typically multiple peaks due to vibrational excitations mixed with the optical transition.

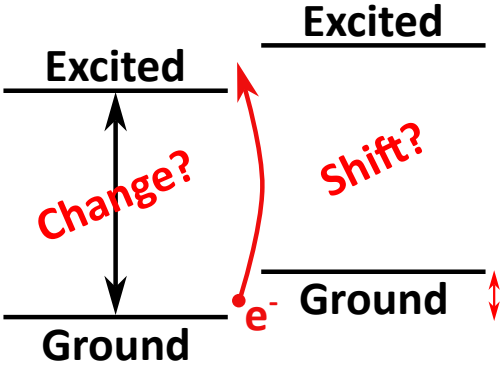

Figure 8: *Tuning of Electron-transfer Properties.*
The energy-levels of the mimic can be tuned in two ways, the ground and excited electron energy-levels can move relative from each other resulting in a change in the energy cap. This would be visible by ultraviolet-visible spectroscopy (UV-VIS). Alternatively, the levels can move synchronously which would be detectable by cyclical voltammetry (CV).

2.2.1 Affirming Metal-Mimic Binding

Titrations describe chemical experiments that determine equivalent concentrations - how much of species X needs to be added to completely react with species Y. For affirming the metal insertion into the crown-ether of the mimic a supramolecular titration by UV-VIS can be conducted. In supramoleular titration a guest species (e.g. metal cations) are incrementally added to host species (e.g. MgCrown) until the used analytical technique ceases to report any changes upon further addition. This helps identify the equivalence needed for complete binding and can be used to determine the binding constant K of guest to host species.

A metal cation M^{n+} binding to a ligand L in a solution (sln) has a chemical equilibrium reaction

$$M^{n+}_{(sln)} + L_{(sln)} \overset{K}{\rightleftharpoons} KM^{n+}_{(sln)}$$

The crown ether (L) of the mimic acts as a cryptand, encapsulating/binding to cations helping mimic the peripheral charge of P680. When varying the metal cation the binding constant K to the cryptand might vary resulting in more or less cations needing to be added to the solution to ensure full insertion. Determining the binding constant can help screen suitable metals for peripheral charge mimicking when designing experiments. Considerations of acidity of the metal is required as Lewis acidity (electron pair accepting) of the cation can lead to substitution of the metal center in the ligand instead of binding to the crown-ether cryptand. For example, previous investigations indicated Sc^{3+} and Al^{3+} were too acidic for titration experiments.[4]. Other cations like K^+ (potassium) were found to be unsuitable due to solubility problems.

The value of the binding constant is affected by the solvent used to dissolve the cation and ligand. Different solvents such as acetonitrile (CH_3CN) or methanol (CH_3OH) will have their own binding constants to the cryptand and thereby compete with the metal cation in binding. Another relevant parameters includes temperature, thus it favour to temperature stabilise the solution during supramolecular titration measurements.

2.2.2 Use of Controls

To ensure any observed response in the MgCrown cryptand is due soley to the presence of cations binding to the crown ether, the measurements are separately conducted under equivalent conditions with MgTPP as control. The difference between the control and MgCrown datasets can then be attributed to the tuning of the electron transfer properties.

3 Experimental Procedure

3.1 Synthesis of H_2TPP

Propionic acid (50 mL) was refluxed with benzaldehyde (1.5 mL, 14.7 mmol) heated to 150 ^{o}C. Pyrrole (1.0 mL, 14.5 mmol) was drop-wise added with the mixture refluxed for 1 h. After cooling the mixture for 30 min. the mixture was vacuum filtered and the residue washed with methanol (40 mL, 3x). The washed residue was dried at 130 ^{o}C for 24 h. yielding H_2TPP (422.4 mg, 19%) ^{1}H NMR (chloroform-d): δ = -2.75 (s, N-H), 1.52 (s, H_2O impurity), 7.26 (s, chloroform solvent), 7.76 (dd & d, *m*-CH & *p*-CH), 8.23 (d, *o*-CH), 8.86 (s, CH_2). IR (ATR): ν/cm^{-1} 3317 (s), interference around 2300.

3.2 Synthesis of MgTPP

H_2TPP (200 mg, 0.325 mmol) was dissolved in DCM (20 mL) and $MgBr_2 \cdot OET_2$ (839.80 mg, 10x equiv). NEt_3 (1 mL) was added and the reaction was mixed for 1 h. Tracking the reaction with a silica TLC a further (420.4 mg, 5x equiv) of $MgBr_2 \cdot OET_2$ and (0.5 mL) of NEt_3 were added leaving the reaction for a further 1 h. Complexation was terminated following a second TLC under UV light indicating incomplete conversion. The mixture was separated using H_2O and DCM and dried in $MgSO_4$. After filtration and rotavaping the solution was dissolved in 20 mL DCM with recrystallisation attempted using 20 mL hexane and cooling for 24 h at -20 °C. After no crystal growth the solution was re-dissolved in excess DCM, rotavaped and separated by aluminate column chromatography with a few drops of NEt_3 in DCM and 5 % methanol. The MgTPP fraction (second eluent) was collected and rotavaped (181 mg, 87 %). ^{1}H NMR (chloroform-d): δ = 0-2 (s, grease impurities), 1.99 (s, acetone impurity), 5.29 (s, DCM impurity), 7.26 (s, chloroform solvent), 7.72 (s, *m*-CH & *p*-CH), 8.21 (s, *o*-CH), 8.85 (s, CH_2). IR (ATR): ν/cm^{-1}, interference around 2300.

3.3 Analysis of MgTPP Control

MgTPP (20 mL, 0.6 mM) was prepared by dissolving 19.1 mg MgTPP in minimal DCM and diluting with CH_3CN. To 2 mL of 0.6 mM of MgTPP, 77.5 mg of $[NBu_4]PF_6$ (0.1 M) and one crystal of $Fe(C_5(C_5H_{15})_2$ was added with titrations conducted against $LiClO_4$ (63.5 mg, 10 mL), $NaClO_4$ (73.5 mg, 10 mL), $Mg(ClO_4)_2$ (113.9 mg, 10 mL), $Ca(ClO_4) \cdot 4\,H_2O$ (376.7 mg, 20 mL) and $Sr(ClO_4) \cdot 3\,H_2O$ (196.4 mg, 10 mL) salts dissolved in CH_3CN. At 300 mV/s scanning rates voltammograms were recorded for 0, 1, 2, 4, 8 and 16 equivalence of salt to MgTPP with 20 µL of salt solution corresponding to one equivalence. UV-VIS were recorded of a 6 and 60 µM MgTPP solution in CH_3CN prepared by diluting the CV MgTPP solutions by ten. Salt solutions (100 mL) were prepared with 20 µL equivalence using the 6 and 60 µM MgTPP solutions. Spectra were collected at 0, 1, 2, 4, 8, 16 and 100 (salt solution) equivalence of salt to MgTPP.

3.4 Analysis of MgCrown

CV and UV-VIS were repeated with the a similar method as the control with 11.6 mg of MgCrown for the CV solution. Protocol differences include halving of equivalences for the Mg_2^+ and Ca_2^+ UV-VIS datasets and including additional equivalences for the CV: 6, 32, 64 and 128. The supramolecular titration against $Mg(ClO_4)_2$ was conducted at 3 and 60 µM MgTPP at the following equivalences: 0 - 2 in steps of 0.1, 2 - 8 in steps of 0.5, 8 - 16 in steps of 1 and 16 - 20 in steps of 4 equivalence of salt.

4 Results

4.1 Synthesis

During H_2TPP synthesis the addition of pyrrole induced a colour change from pale yellow to red/brown to black/brown. Metalation to MgTPP involved two colour changes: red to green after adding Mg^{2+} and green to purple after adding NEt_3. ^{1}H NMR confirms traces of acetone, grease and DCM were introduced with the removal of water and chloroform impurities. The IR further confirms both H_2TPP and MgTPP contained negligible water content (Fig. 9).

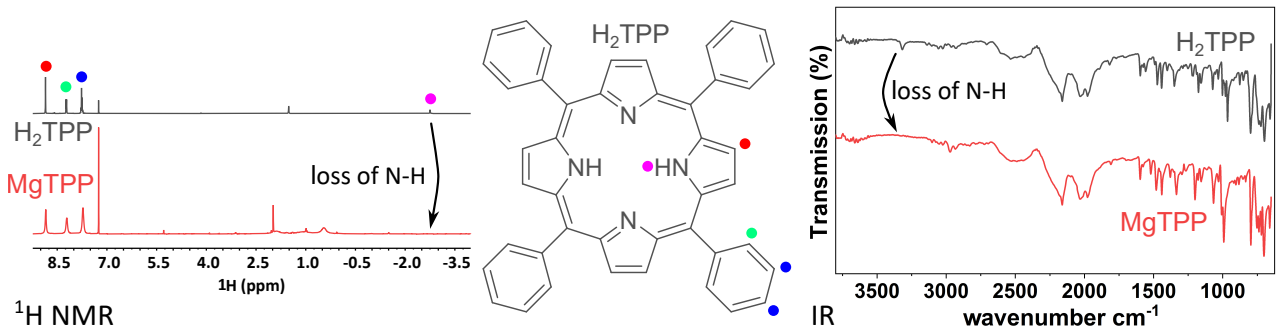

Figure 9: *^1H NMR and IR of H_2TPP and MgTPP.*
Tracking the loss of the N-H bond using ^{1}H NMR and IR in metalating H_2TPP to MgTPP. The ^{1}H NMR proton environments matches the proton environments (and number of protons per environment by integration) for H_2TPP with the MgTPP NMR not being sufficiently resolved but agreeing on the integration.

4.2 MgTPP Control

The measured UV-VIS spectra at 6 (S) and 60 (Q) μM are shown for the +1 and +2 cations respectively in figures 10 and 11. S and Q bands were located at 421 ± 1, 563 ± 1 and 602 ± 1 nm for all the spectra per cation dataset.

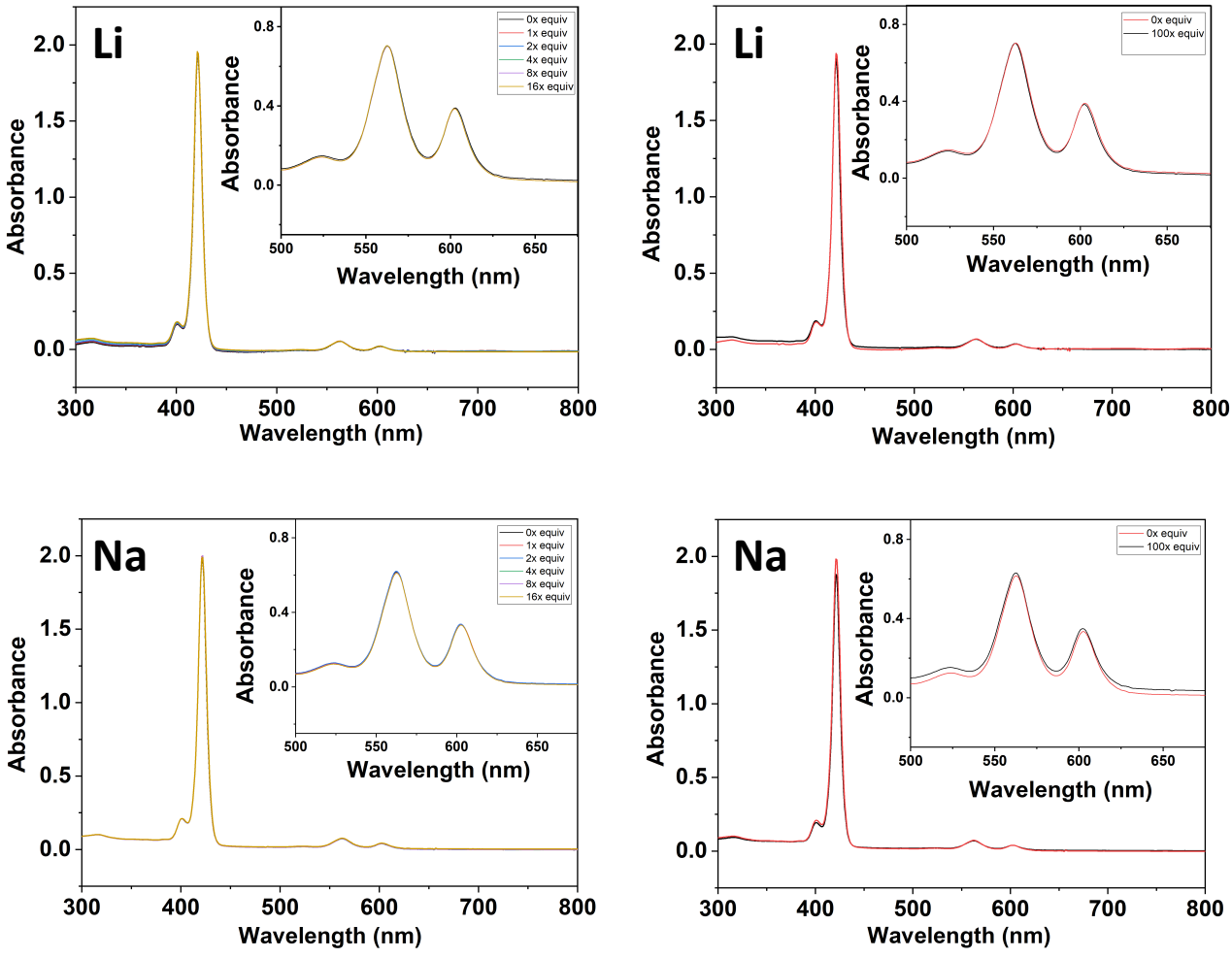

Figure 10: *MgTPP Control UV-VIS against +1 Metal Cations.*
UV-VIS data for the S and Q bands of MgTPP against Li^+ and Na^+.

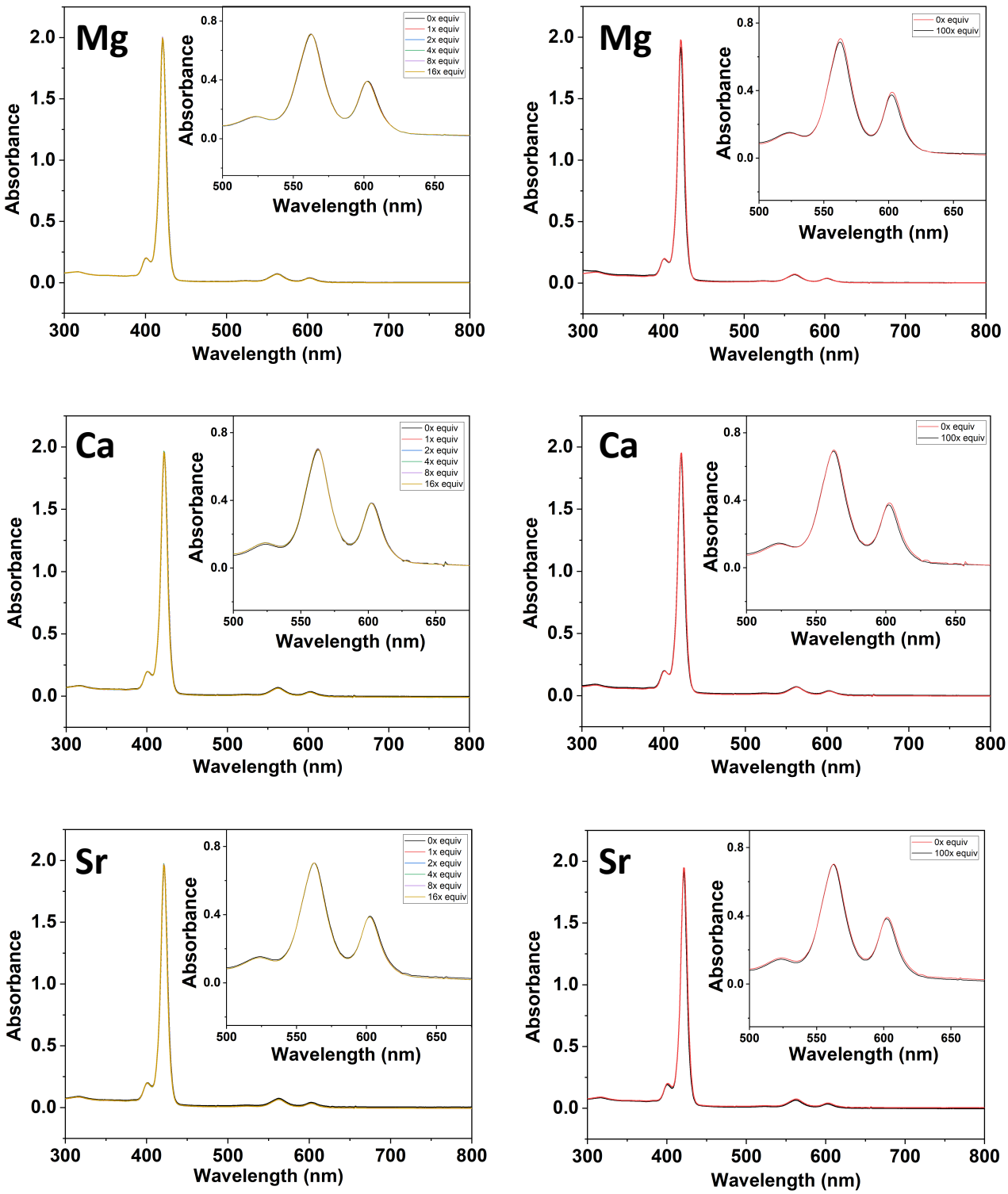

Figure 11: *MgTPP Control UV-VIS against +2 Metal Cations.*
UV-VIS data for the S and Q bands of MgTPP against Mg^{2+}, Ca^{2+} and Sr^{2+}.

The CV data and corresponding half-potential estimate for the redox potential for the +1 and +2 cations respectively are shown in figures 12 and 13.

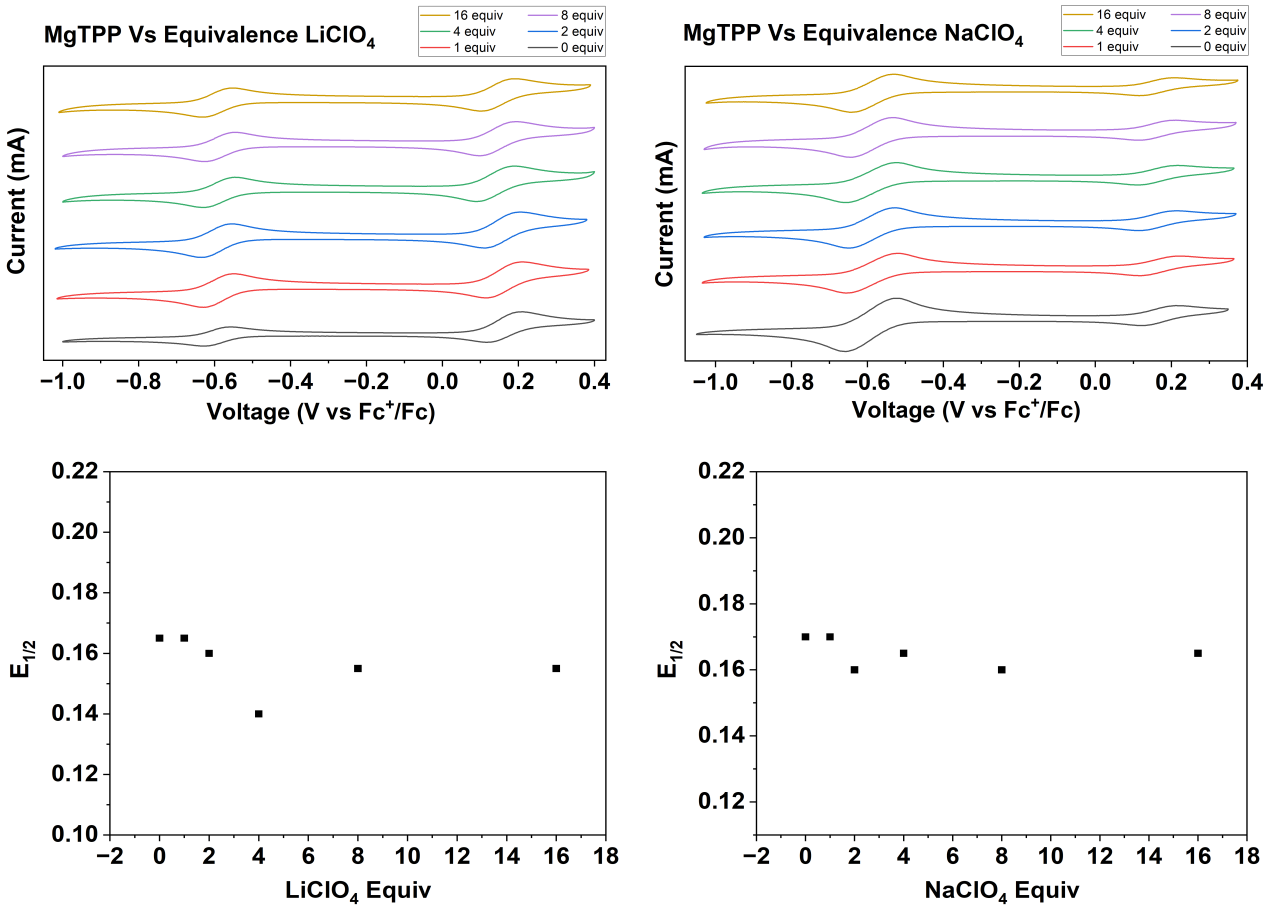

Figure 12: *MgTPP Control CV against +1 Metal Cations.*
(Above) CV data of MgTPP against Li^+ and Na^+. (Below) the calculated half-potential $E_{1/2}$ approximation for the redox potential E^o.

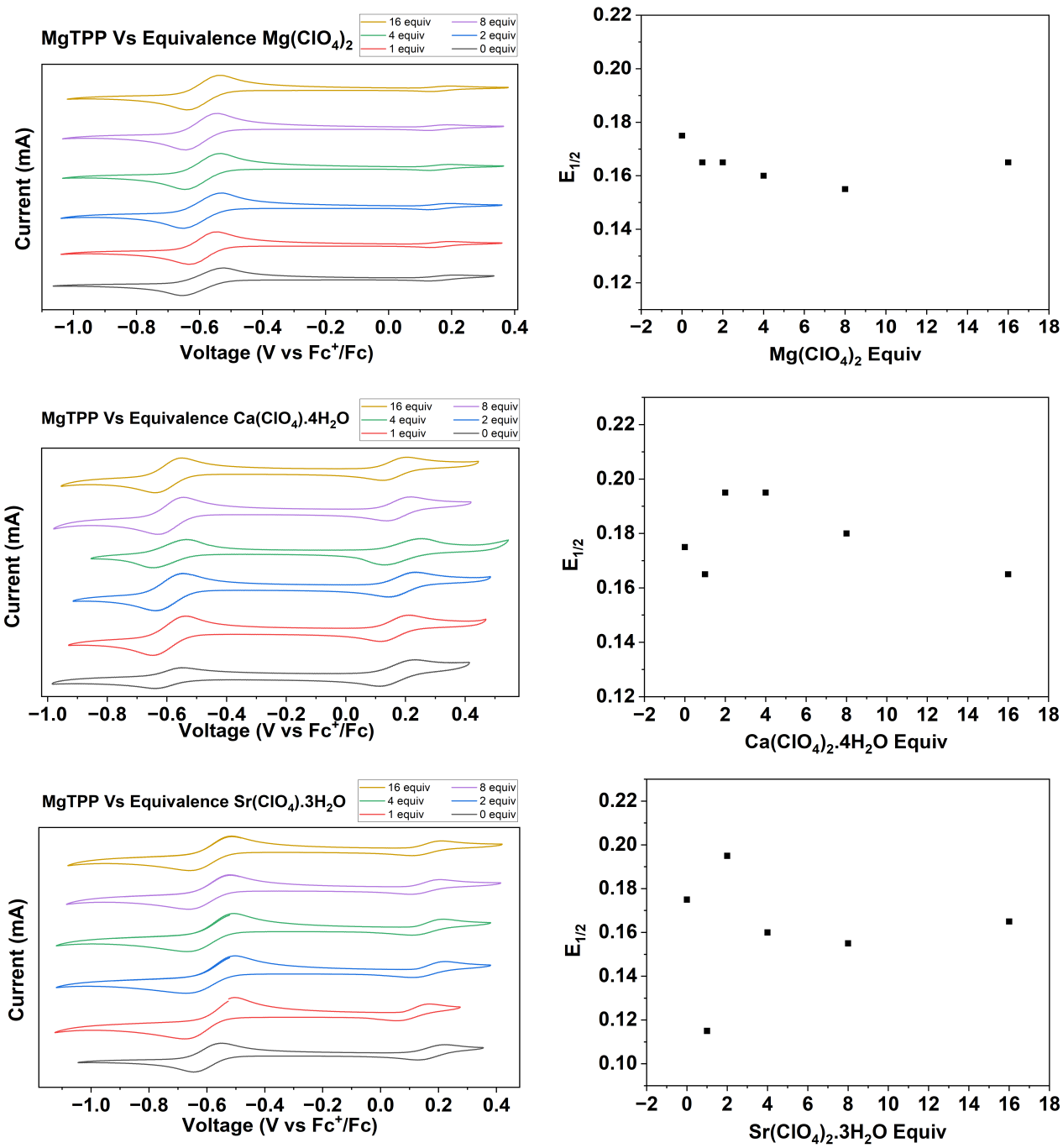

Figure 13: *MgTPP Control CV against +2 Metal Cations.*
(Left) CV data of MgTPP against Mg^{2+}, Ca^{2+} and Sr^{2+}. (Right) the calculated half-potential $E_{1/2}$ approximation for the redox potential E^{o}.

4.3 MgCrown

The measured UV-VIS spectra at 6 (S) and 60 (Q) μM are shown for lower and higher cation equivalence respectively in figures 14 and 15.

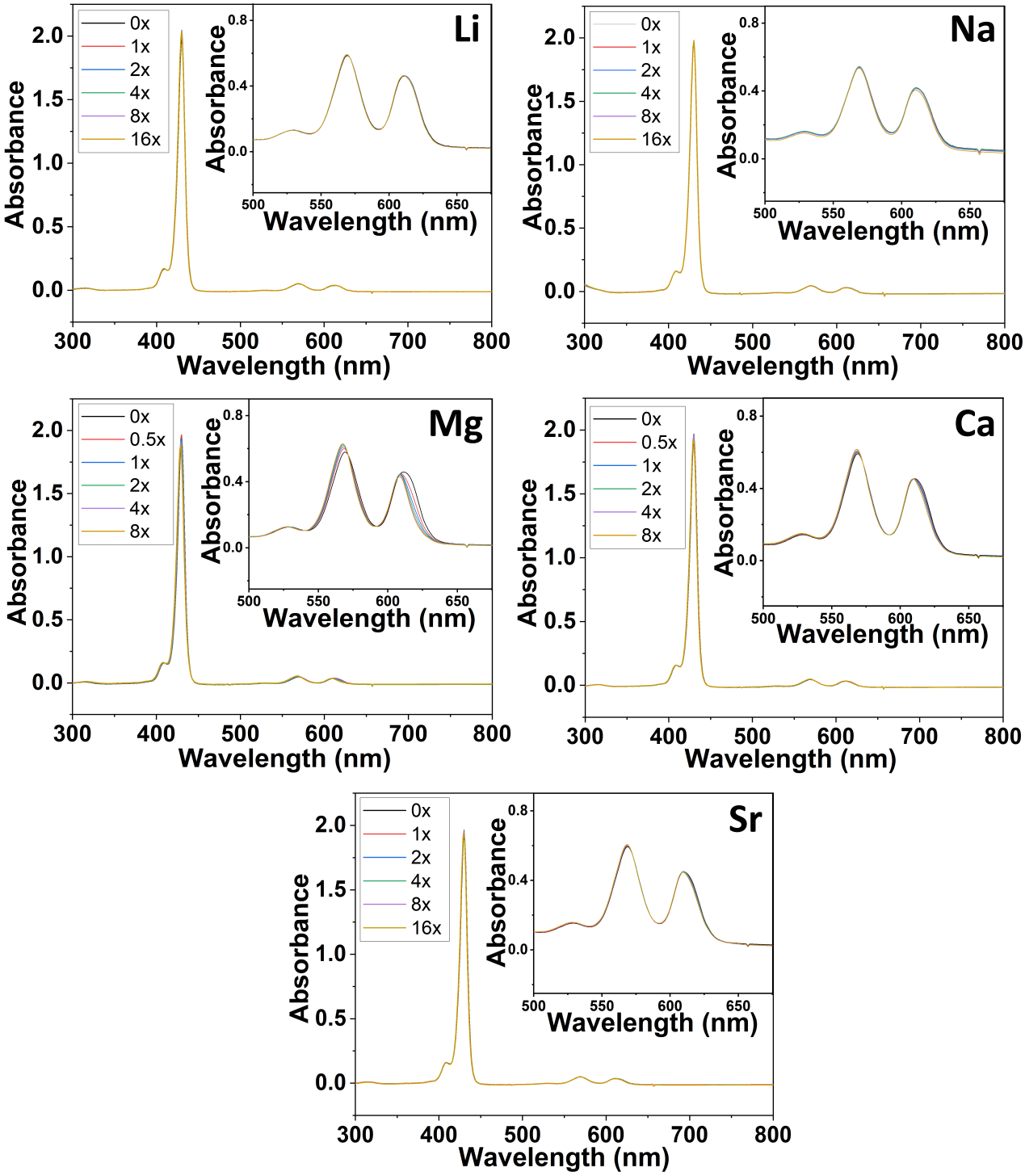

Figure 14: *MgCrown UV-VIS against at lower equivalence.*
UV-VIS data for the S and Q bands of MgCrown against Li^+ and Na^+ up to 8 or 16 equivalence.

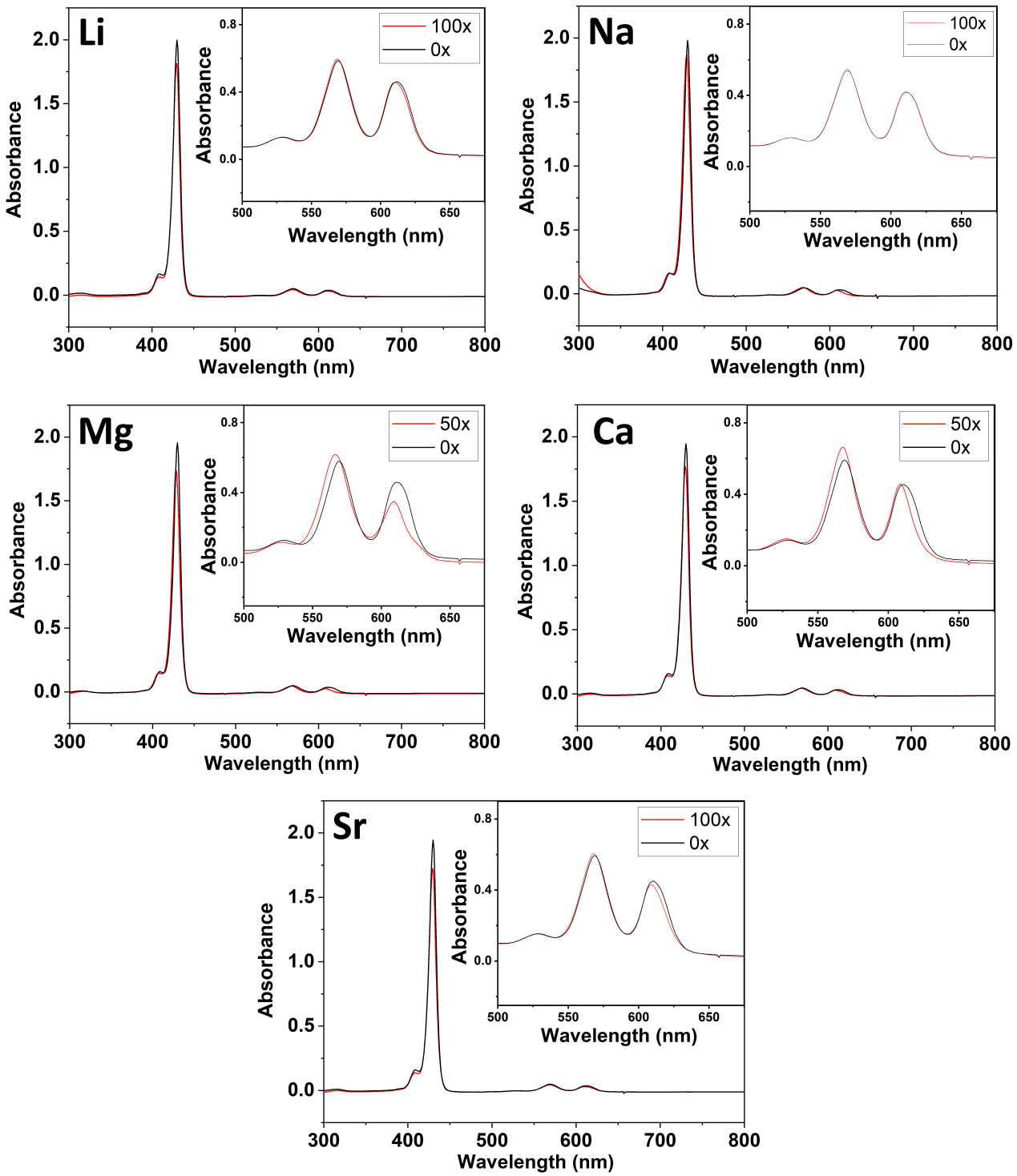

Figure 15: *MgCrown UV-VIS against at higher equivalence.*
UV-VIS data for the S and Q bands of MgCrown against Mg^{2+}, Ca^{2+} and Sr^{2+} up to up to 50 or 100 equivalence.

The CV data for the +1 and +2 cations respectively are shown in figures 16 and 17. Figure 18 compares the MgTPP control and the MgCrown to the highest titration equivalence.

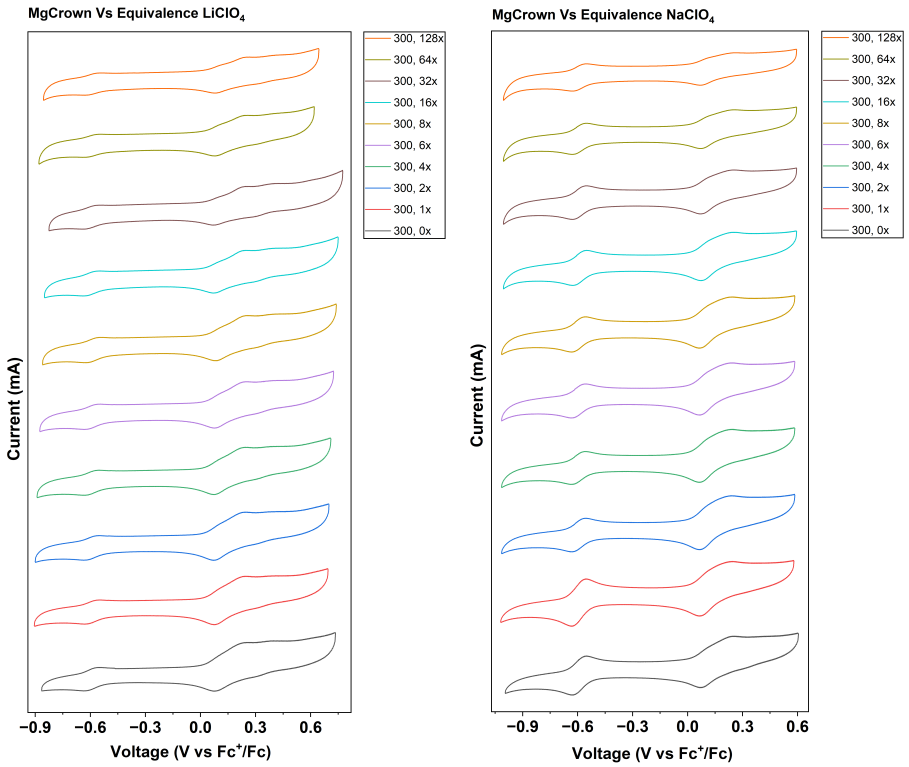

Figure 16: *MgCrown CV against +1 Metal Cations.*
CV data of MgCrown against Li^+ and Na^+.

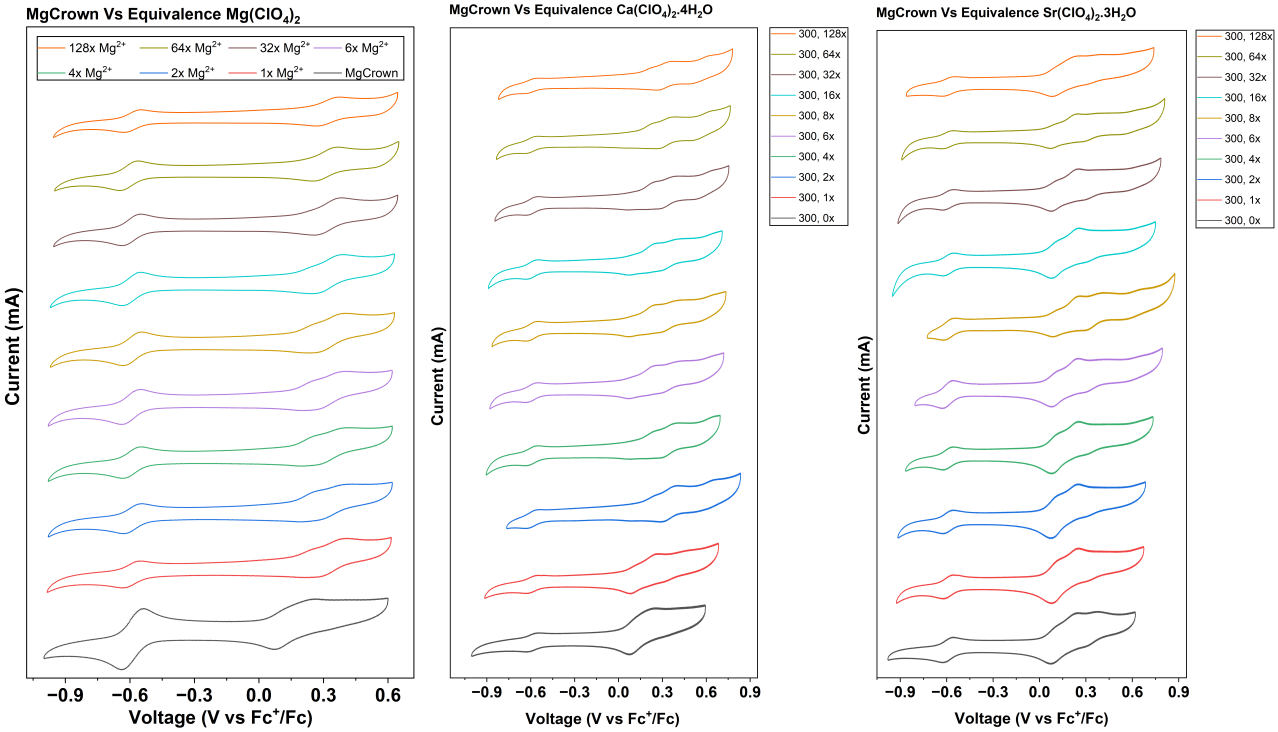

Figure 17: *MgCrown CV against +2 Metal Cations.*
CV data of MgCrown against Mg^{2+}, Ca^{2+} and Sr^{2+}.

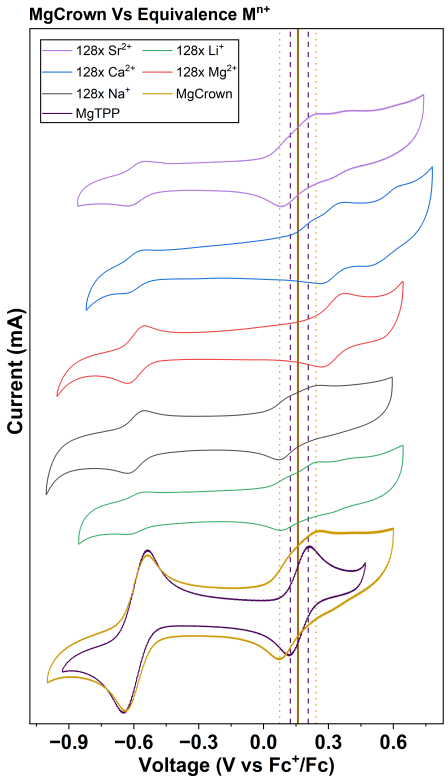

Figure 18: *MgCrown CV at high equivalence.*
CV data of MgCrown at high equivalence against the MgTPP coontrol and MgCrown.

The supramolecular titration against magnesium is shown in figure 19 including the global fits on the Q bands. The standard fitting method set by Thordarson et. al. was implemented.[9]

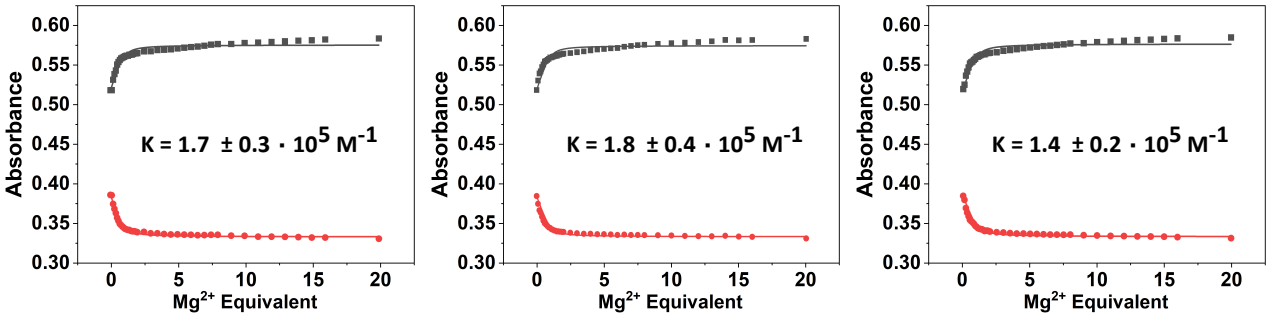

Figure 19: *Supramolecular Mg^{2+} Titration Fits to Q.*
Binding constant K estimation through global fitting of the Mg^{2+} titration of the Q bands of MgCrown chlorophyll mimic.

5 Discussion

5.1 Synthesis

The observed colour changes during the synthesis of H_2TPP are consistent with the formation of longer polymers as side-products. The observed yield of 19 % is consistent with the literature (20 %).[5] Literature yields for this reaction under the same conditions differ wildly including reported yields of 7 % and 90 % indicating the reaction is sensitive to subtle changes in conditions.[6,7]

The red to green colour change after adding Mg^{2+} to H_2TPP illustrates the coordination of the cation prior to the displacement of protons inside the porphyrin ring. The UV-VIS spectra shifts due to the presence of the cations, similar to the peripheral charge effect investigated in this work. The subsequent addition of the NEt_3 (base) inducing the colour change to purple is consistent with the deprotonation of the acidic N-H protons to form MgTPP. The metalation to MgTPP is reported to have a yield of 100 % using MgI_2 which is coarsely consistent with the observed yield of 87 %.[8]

5.2 MgTPP Control

Figures 10 and 11 indicate the optical transitions aren't affected by the perchlorate salts. The perchlorate anion is therefore a spectator ion and the MgTPP control mimic inert to peripheral cation's effect on is ground to excited energy levels spacing. The 0 to 100 equiv datasets are also similar showcasing the measurement was reliable. Similarly figures 12 and 13 indicates the redox potential is unaffected by the salts, affirming the selection of the MgTPP mimic to control as appropriate.

5.3 MgCrown

From figures 14 and 15 a trend is observed, 2+ cations reveal a larger perturbation in the Q bands than +1 cations with the perturbation decreasing for Sr. This is consistent with higher charge densities giving rise to larger ET tuning as the atomic radius increases down a period (row on the periodic table). A similar trend is observed for the redox potential in figures 16 and 17 with a noticeable shift observed only for smaller radius +2 cations. Figure 18 highlights this trend by highlighting the overlap of the MgTPP and MgCrown redox potential to the titration end-voltammograms per salt. The complex envelope of the voltammogram at lower equivalence is hard to interpret but appears to simplify upon addition of excess metal cations. Apart from Mg the other metal titrations appear not to have reached full binding to the cryptand indicating a lower binding constant to these metal cations. For magnesium the binding constant is estimated at $\log(K) = 5.2 \pm 0.1$ considering the fit values from figure 19. The fits might improve by truncating the data to exclude higher equivalences as the fractional error at this datapoints could exceed the signal variation induced by the titration.

Along a period the binding constant K tends to increase in similar cryptands.[10] Down a group (column in periodic table) K tends to increase also.[11] The trends follow in part because of the fitting of the cation into the crown-ether of the cryptand, a 4,13-diaza-18-crown-6 ether for the mimic.[12] Higher charges (along period) have stronger affinity for the cryptand with larger cations (down group) fitting more appropriately in the cryptand favouring bond formation through greater orbital overlap. This trend becomes evident when comparing the size of the hole in the cryptand (1.4 Å) to the radius of the cations ($\sim$ 1 Å).[13].

The drop in binding peaking dropping from Mg to Sr observed in this work is different from the literature and might be affected by the bending of the cryptand. The MgCrown mimic (Fig. 3) is expected to have an oval shape and might also bend due due to sterics from the proximity to the porphyrin ring. The introduction of a cation into the cryptand might induce further conformational changes in the molecule that might explain the simplification of the voltammograms at higher equivalences and drop in binding after Mg. ^{1}H NMR titration could be used to verify the binding of the metal with the cryptand with further X-ray crystallography revealing geometrical distortions in MgCrown. Repeating the measurements using cryptands of larger and smaller ring sizes provides a further approach to test this hypothesis.

In previous work a +4 cation near a chlorophyll mimic with a larger charge-to-mimic distance than the MgCrown of this work produced a redox potential shift of 80 mV. Using a +2 cation figure 18 showcases a shift of 170 mV, more than doubling the previously observed trend. For chlorophyll-*a* the redox potential shift of 500 mV might thus be achievable using charges with a smaller charge-to-chlorophyll distance, showcasing how peripheral charges could play a significant role in enabling the chemistry of PSII.

6 Conclusion

Tetraphenylporphyrin (H_2TPP, 19 %) was synthesised with high purity and yields consistent with the literature.[5] Metalation of the product into magnesium tetraphenylporphyrin (MgTPP, 87%) was observed with high purity and yields in coarse agreement with the literature.[8] Ultraviolet-Visible Spectroscopy (UV-VIS) and Cyclical Voltammetry (CV) showed no significant tuning of the electron transfer (ET) properties of MgTPP with titrations against perchlorate salts of Li, Na, Mg, Ca and Sr. The MgCrown mimic with the crown-ether cryptand revealed a trend of higher charge density, demonstrating a larger shift in redox potential and perturbation in optical transitions. Variation in the binding of the metal cations are suspected to affect the results with partial insertion expected for all datasets excluding Mg. Literature findings show an opposite trend in binding constants to the observed trend which could be explained by conformational perturbations in MgCrown that might affect binding trends.[10,11,12,13] The trend in redox potential in MgCrown resulted in a shift of 170 mV, more than doubling previous work of chlorophyll-*a* mimics using a smaller peripheral charge.[4] Thus 34 % of the 500 mV redox potential shift seen in P680 can be explained using peripheral charge effects showcasing the significance of the Stark effect on reactivity, further optimisation could increase that fraction and possibly unlock water splitting and more novel chemistry.

A Research Reflections

According to Murphy's law, anything that can go wrong will go wrong. This was definitely the case in this project from instrumentation misbehaving to synthesis failures. The weeks spent on synthesising NiTPP to study the effects of covalent over ionic bonding for example isn't covered in this report as isolating the product proved challenging. Knowing to prioritise and keeping calm whilst sounding trivial I've found to make or break an endeavour like this one.

The importance of a network to rely on is another trivial sounding statement that deserves to be emphasised. Different insights, suggestions and experiences catalyse progress and can be assuring mentally when coping with a conundrum. The attendance to community events, learning beyond the exact topic being studied further helped me narrate the story of this research and appreciate the paradigm our understanding currently rests. If I have to summarise in a sentence what leadership skills I noticed the strongest it is patience, endurance and kindness when working in a team - something I got to appreciate a lot during this research project.

B Events Attended

Group Meetings
These meetings summarised the recent progress made by group members working on Porphyrin chemistry. Discussed feedback, troubleshooting and suggestions.

- 24/06/2025 (Presenter and spectator)
- 07/07/2025 (Presenter and spectator)
- 21/07/2025 (Presenter and spectator)
- 18/08/2025 (Presenter and spectator)
- 02/09/2025 (Presenter)
- 30/06/2025 (Presenter and spectator)
- 14/07/2025 (Presenter and spectator)
- 08/08/2025 (Presenter and spectator)
- 22/08/2025 (Presenter)

Literature Reviews
These meetings involved presenting relevant research articles to the research topics of the research group. Long-term research progress by members was also presented.

- 02/07/2025 (Spectator)
- 16/07/2025 (Spectator)
- 06/08/2025 (Spectator)
- 18/08/2025 (Spectator)
- 20/08/2025 (Spectator)
- 09/07/2025 (Spectator)
- 23/07/2025 (Spectator)
- 18/08/2025 (Spectator)

Action Learning Set
Meeting with four other TCD Laidlaw Scholars to discuss issues and work towards solutions for them - in real time.

- 03/07/2025 (Facilitator)
- 05/08/2025 (Presenter)
- 19/08/2025 (Member)

Seminars

- 25/06/2025 (Spectator): ACS-RSEQ - Global Inorganic Virtual Seminars
- 30/06/2025 (Spectator): 300 Years of Chemistry Launch Event

C Acknowledgements

This research was funded by the Laidlaw Foundation through the Laidlaw Scholars Leadership and Research Programme and the McDonald Research Group at the School of Chemistry, Trinity College Dublin (TCD). Prof. Aidan R. McDonald and Oscar R. Kelly supervised the project with O. Kelly providing training and synthesising the novel MgCrown mimic. Plentiful of guidance was provided by the other members of the McDonald research group. The IR and NMR instrumentation facilities used in this work were provided by the School of Chemistry.

D Declaration

I have read and understood the plagiarism provisions in the General Regulations of the University Calendar for the current year, found at http://www.tcd.ie/calendar.

I have also read and understood the guide, and completed the 'Ready Steady Write' Tutorial on avoiding plagiarism, located at https://libguides.tcd.ie/academic-integrity/ready-steady-write.

Supervisor: *Prof. Aidan McDonald* Co-Supervisor: *Oscar Reid Kelly*

References

[1] J. P. McEvoy & G. W. Brudvig, *Chem. Rev.*, **106**, 11, 2006, p. 4455 – 4483.

[2] *RCSB Protein Data Bank*, https://www.rcsb.org/structure/7NHP, last accessed: 11/09/2025.

[3] S. A. Siddiqui, T. Stuyver, S. Shaik & D. Dubey, *JACS Au*, **3**, 12, 2023, p. 3259 – 3269.

[4] O. R. Kelly, B. Twamley, M. Swart & A. R. McDonald, *J. Am. Chem. Soc.*, **147**, 32, 2025, p. 29399 – 29412.

[5] S. Ajit, S. Palaniappan & P. U. Kumar, P. Madhusudhanachary, *J. Pol. Sci. Part A: Polymer Chemistry*, **50**, 5, 2012, p. 884 - 889.

[6] Y. Aqeel, R. Siddiqui, A. Anwar, M. R. Shah, S. Khoja & N. A. Khan, *Antimic. Ag. Chemo.*, **59**, 6, 2015, p. 3031 - 3041.

[7] S. Sakthinathan, S. Kubendhiran, S-M. Chen, M. Govindasamy, F. M.A. Al-Hemaid, M. A. Ali, P. Tamizhdurai & S. Sivasanker, *J. App. Org. Chem.*, **31**, 9, 2017, e3703.

[8] K. Tanaka, G. Pescitelli, K. Nakanishi & N. Berova, *Chemical Monthly*, **136**, 3, 2005, p. 367 – 395.

[9] P. Thordarson, *Chem. Soc. Rev.*, **40**, 3, 2011, p. 1305 - 1323.

[10] H. Tsukube, K. Yamashita, T. Iwachido & M. Zenki, *J. Org. Chem.*, **56**, 1, 1991, p. 268 – 272.

[11] V. J. Gatto & G. W. Gokel, *J. Am. Chem. Soc.*, **106**, 26, 1984, p. 8240 – 8244.

[12] H-J. Buschmann, *J. Sol. Chem.*, **15**, 6, 1987, p. 181 – 190.

[13] A. D'Aprano & B. Sesta, *J. Phys. Chem.*, **91**, 9, 1987, p. 2415 – 2422.